Taxus baccata (L.) leaves extract as eco-friendly corrosion inhibitor for mild steel in 1 M HCl: GC/MS, electrochemical, SEM/EDX analysis and DFT studies

Ouassima Riffi (ouassimariffi95@gmail.com)
Moulay Ismail University
Elhachmia Ech-chihbi
University Sidi Mohamed Ben Abdellah
Rajae Salim
University Sidi Mohamed Ben Abdellah
Mustapha Taleb
University Sidi Mohamed Ben Abdellah
Jamila Fliou
Moulay Ismail University
Ali Amechrouq
Moulay Ismail University

Research Article

Keywords: Taxus baccata (L.), GC/MS, corrosion inhibition, adsorption process, surface morphology, DFT

Posted Date: November 11th, 2022

DOI: https://doi.org/10.21203/rs.3.rs-2248337/v1

Additional Declarations: No competing interests reported.

Taxus baccata (L.) leaves extract as eco-friendly corrosion inhibitor for mild steel in 1 M HCl: GC/MS, electrochemical, SEM/EDX analysis and DFT studies

Ouassima Riffi[1], Elhachmia Ech-chihbi[2], Rajae Salim[2], Mustapha Taleb[2], Jamila Fliou[1], Ali Amechrouq[1]

[1]*Laboratory of Molecular Chemistry and Natural Substance, Moulay Ismail University, Faculty of Science, B.P. 11201 Zitoune, Meknes, Morocco*

[2]*Engineering Laboratory of Organometallic, Molecular Materials, and Environment, Faculty of Sciences, University Sidi Mohamed Ben Abdellah, Fez, Morocco*

**Corresponding author e-mail address: ouassimariffi95@gmail.com*

Abstract

This study aims at the valorization of *Taxus baccata* (L.) in corrosion inhibition. The effect of the extract on corrosion inhibition of mild steel in 1.0 M HCl solution by weight loss measurements, potentiodynamic polarization (PP) and electrochemical impedance spectroscopy (EIS) showed that *Taxus baccata* (L.) leaves extract is a good corrosion inhibitor with an inhibition efficiency of 98%, 96% and 95% at the concentration of 1.0 g/L respectively. Polarisation curves indicated that the extract acted as a mixed type inhibitor. The adsorption on the mild steel surface obeyed the Langmuir isotherm. The activation energy values ΔG^0_{ads} (-29.61 KJ.mol^{-1}) confirmed the physical adsorption process of this inhibitor. The study of adsorption kinetics showed a maximum inhibitory efficiency of 90.5 % after one hour of immersion time. Scanning electron microscopy revealed the formation of a protective layer on the steel surface. Analysis of the extract by gas chromatography revealed the dominance of Diisooctyl phthalate (17.22%), Bicyclo [4.4.0] dec-2-ene-4-ol,2-methyl-9-(prop-1-en-3-ol-2-yl) (16.43%), Methanesulfonic acid,4-oxoadamantan-2-yl ester (8.75%), Diethyl phthalate (8. 31 %), The structural and electronic properties of the main components of this extract were calculated using DFT to better understand the adsorption behaviour and inhibition mechanism of this plant.

Keywords: *Taxus baccata (L.)*; GC/MS; corrosion inhibition; adsorption process; surface morphology; DFT.

1. Introduction

The study of corrosion is one of the most important subjects in chemistry. Because of the direct and indirect damage caused by this phenomenon. Economically, more than a quarter of the world's steel production is damaged due to corrosion **[1]**. Mild steels in general are susceptible to corrosion over time, which can be quite dangerous and reduce the life of the steels themselves. The use of corrosion inhibitors as a means of protection is necessary in many industrial cases: surface preparation, transport and storage of metals, cooling systems, rehabilitation of reinforced concrete, painting and cathodic protection. The current trend is towards synthetic inhibitors and green or environmentally friendly inhibitors **[2,3]**. Most of the synthetic compounds have good anticorrosive action, but the majority of them are highly toxic to humans and the environment. Indeed, these inhibitors can cause temporary or permanent damage to certain organs such as the kidneys or liver and can even disrupt the enzyme system in the body **[4]**. Therefore, due to the hazardous effects of synthetic inhibitors, plant extracts are increasingly being considered as a source of highly effective and environmentally friendly green corrosion inhibitors **[5]**. In recent years, more and more corrosion specialists have started to investigate green organic corrosion inhibitors, such as *Taxus baccata* (L.), which is a needle-leaved evergreen tree belonging to the Taxaceae family. It is a slow-growing, long-lived tree **[6]**. *Taxus baccata* (L.) is little known in traditional medicine. However, due to other active substances with very important physiological activities, this plant is well known in pharmacy and medicine. Active substances in plants of the genus Taxus, such as lignans, steroids and flavonoids and other phenolic components, have antibacterial and antifungal activity **[7,8]**, enzyme inhibitory and antioxidant activity **[9]**, anticancer activity **[10,11]** and insecticidal activity **[12]**. An anticancer substance extracted from the Taxus species, Taxol (Paclitaxel), has been discovered in the bark of the Pacific yew (Taxus brevifolia Peattie) **[13]**, It is often used in chemotherapy for lung, ovarian and breast cancer **[14]**.

The present work is devoted to the study of the chemical composition of *Taxus baccata* (L.) extract and its ability as a corrosion inhibitor of mild steel in a molar hydrochloric acid medium by applying different experimental techniques: weight loss, potentiodynamic polarization curves and electrochemical impedance spectroscopy (EIS), The study of the morphology of mild steel by scanning electron microscope coupled with EDX spectrometer. This study was complemented by a complementary theoretical approach using density functional theory (DFT) at B3. Density functional theory (DFT) at B3LYP/6-31G (d, p).

2. Materials and methods

2.1. Plant material

The plant material used in our study is the aerial part of *Taxus baccata* (L.) harvested in March 2019 in the IFRANE forest (Latitude: 31.7021700°, Longitude: -6.3494000°) in MOROCCO. The plant was dried in a dry and ventilated place for 1 month, ground with an electric mill and kept in the shade in closed jars. 50 g of plant powder was placed in a cartridge, then placed in a siphon attached to a flask containing 250 mL of extraction solvent (methanol). The whole is topped with a refrigerator. After 6 hours of extraction, the solvent was then evaporated using a rotary evaporator, the extract obtained was considered to be the crude extract of our plant.

2.2. Gas chromatography/mass spectroscopy (GC/MS)

GC/MS analyses were performed using the Thermo Scientific ISQ Series quadrupole GC-MS system. Equipped with a TG-1MS capillary column (30 m × 0.32 mm i.d., film thickness 0.25 µm). The carrier gas used was helium (He) with a flow rate of 1.5 ml/min and an EI source at 70 eV. The GC oven was maintained at a temperature of 40°C at the initial time and programmed to 200°C at 4°C/min and up to 300°C at 30°C/min and maintained for 10 min. 1µl of the diluted sample (in 1:100 cyclohexane, v/v) was injected at a constant temperature of 250°C through a split injector. The identification of chemical components was performed by comparing the Chemical Abstract Service (Cas) registry number and matching their mass spectrum value with the corresponding NIST database and mass spectrum literature (the Reverse Match Factor RSI > 600) **[15, 16]**.

2.3. Preparation of the materials

The steel used in the present work is mild steel consisting of Fe (99.21), C (0.21), Mn (0.05), Si (0.38), S (0.05), P (0.09) and Al (0.01). The aggressive 1.0 M HCl solution was prepared by diluting 37% analytical grade HCl with distilled water. The concentration range of the studied inhibitors was (0.25 g/L- 1.0 g/L).

2.4. Weight loss study

Weight loss experiments were carried out in a double-walled glass cell equipped with a thermostatic cooling condenser, the samples were accurately weighed and immersed in beakers containing 100 ml of acid solutions without and with inhibitor (the studied extract) at different temperatures for 6 hours. The inhibitory efficiency was calculated according to the Eq. (1):

$$\eta_{\mathrm{WL}}(\%) = \left[\frac{C_R^{\circ} - C_R}{C_R^{\circ}} \right] \times 100 \qquad (1)$$

where C°_R represents the weight loss of mass in the absence of the inhibitor and C_R is the weight loss of mass in the presence of the inhibitor

2.5. Electrochemical measurements

Electrochemical experiments were carried out using a Versa STAT 4 potentiostat, controlled with versa studio software. A three-electrode cell with Pt as a counter electrode, Ag/ AgCl as reference electrode and a carbon steel working electrode with a surface area of 1.0 cm^2 was used for these measurements. To reach the steady-state, before each experiment, the potential was stabilized at the free potential for 30 min. Polarization curves were performed with a scan rate of 1.0 $mV.S^{-1}$ with a potential range of ±250 mV at the open circuit potential (OCP). The inhibition efficiency ($\eta_{pp}\%$) was calculated from the corrosion current density values using Eq. (2) **[17]**.

$$\eta_{pp}\% = \left[i^{\circ}_{corr} - i_{corr} \Big/ i^{\circ}_{corr} \right] \times 100 \qquad (2)$$

where i°_{corr} represents the corrosion current density value in the absence of inhibitor and i_{corr} is the corrosion current density value in the presence of inhibitor

The Electrochemical impedance spectroscopy (EIS) measurements were carried out using alternating signals of amplitude 10 mV peak-to-peak at different conditions in the frequency range from 100 kHz to 10 mHz. The inhibition efficiency was calculated using Eq. (3) **[18]**.

$$\eta_{imp}\% = \left[R'_p - R_p \Big/ R_p \right] \times 100 \qquad (3)$$

where R'_p represents the polarization resistance of the mild steel electrode in the presence of inhibitor and R_p is the polarization resistance of the mild steel electrode in the absence of inhibitor

2.6. Scanning electron microscope

The surface morphology of the steel samples was obtained after immersion in the studied solutions (with or without inhibitor) using the JSM-IT 500 HR SEM technique connected to an X-ray analysis system (EDX) using 8 KV electron acceleration to determine the elemental composition of the surface of the samples.

2.7. Computational investigation

DFT method using B3LYP with 6-311G(d,p) was undertaken to investigate the electronic structure of molecules. The FMOs and DFT descriptors were determined utilizing Gaussian 09 **[19]**. Four major molecules of the studied extract, namely, Bicyclo[4.4.0]dec-2-ene-4 -ol,2-methyl-9-(prop-1-en-3-ol-2-yl) (**A**), Diisooctyl phthalate (**B**), Methanesulfonic acid,4-oxoadamantan-2-yl ester (**C**) and Diethyl Phthalate (**D**) have been computationally investigated in the aqueous phase. In this regard, the effect of solvents (water) was included in all DFT computations employing the using integral equation formalism variant of the Polarizable Continuum Model (IEFPCM) **[20]**. A variety of DFT descriptors (e.g., HOMO and LUMO energies, gap energy (ΔE_g), global softness (σ), back donation energy ($\Delta E_{b\text{-}d}$), chemical electronegativity (χ) and the fraction of electrons transferred (ΔN) were evaluated using the following equations **[21, 22]**:

$$\Delta E_{gap} = E_{LUMO} - E_{HOMO} \tag{4}$$

$$\sigma = \frac{1}{\eta} \tag{5}$$

$$\eta = \frac{1}{2}\left(E_{HOMO} - E_{LUMO}\right) \tag{6}$$

$$\chi = \frac{1}{2}\left(E_{HOMO} + E_{LUMO}\right) \tag{7}$$

$$\Delta N_{110} = \frac{\chi_{Fe(110)} - \chi_{inh}}{2\left(\eta_{Fe(110)} + \eta_{inh}\right)} = \frac{\Phi - \chi_{inh}}{2\eta_{inh}} \tag{8}$$

Fukui indices are important to recognize the reactive centers of electrophilic and nucleophilic within the same molecule **[23]**. It's calculated according to equations (9) and (10) **[24,25]**.

$$f_k^+ = P_k(N+1) - P_k(N) \text{ for Nucleophilic attack} \tag{9}$$

$$f_k^- = P_k(N) - P_k(N-1) \text{ for Electrophilic attack} \tag{10}$$

Where P_k (N) P_k (N + 1), P_k (N-1), are the neutral, anionic and cationic of the molecule, respectively. The Mulliken Population Analysis (NPA) has been used to express Fukui functions in the present study.

3. Results and discussion

3.1. Gas chromatography/mass spectroscopy (GC/MS)

The chromatogram corresponding to the extract of *Taxus baccata* (L.) is given in Fig. 1.

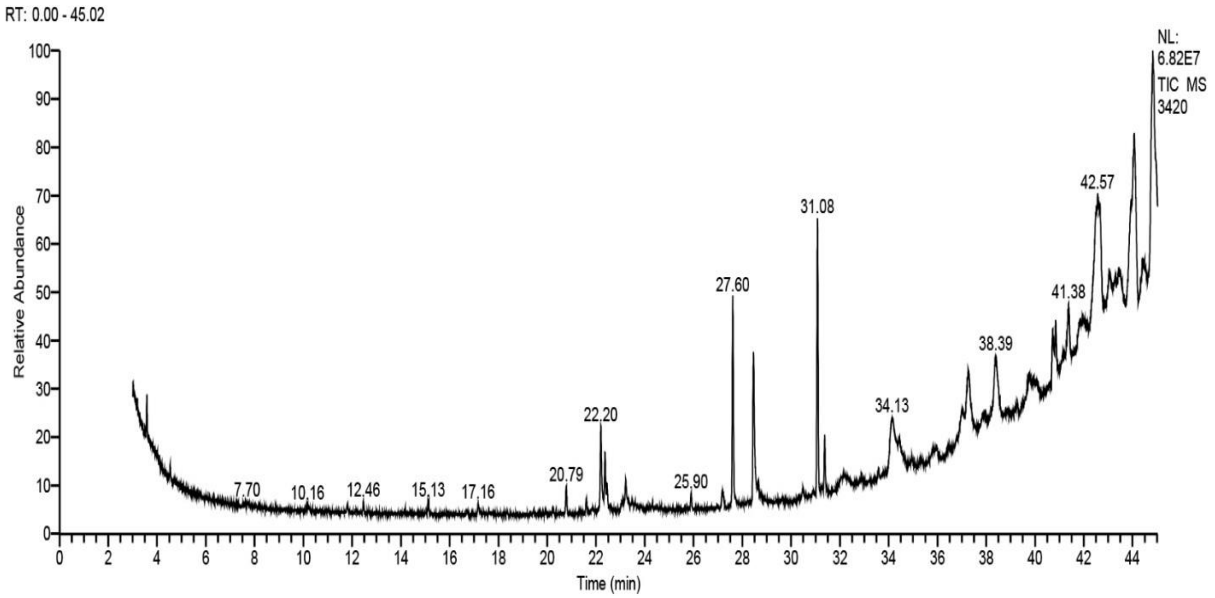

Fig.1 Chromatogram of the methanolic extract of *Taxus baccata* (L.)

The chemical composition of the methanolic extract of *Taxus baccata* (L.) revealed major compounds such as Diisooctyl phthalate (17.22 %), Bicyclo[4.4. 0]dec-2-ene-4 -ol,2-methyl-9-(prop-1-en-3-ol-2-yl) (16.43 %), Methanesulfonic acid,4-oxoadamantan-2-yl ester (8.75 %), Diethyl phthalate (8.31 %), 2(3H)-Furanone, 5-hexyldihydro (6.2 %). The identification of the chemical composition of Taxus baccata (L.) has been the subject of several studies over the years **[26,27]**.

The molecules found in the chromatogram are presented in Table below:

Table 1. Majority molecules of the methanolic extract of *Taxus baccata* (L.)

Constituants	**Formula**	**RT**	**Percentage**
Toluene	C_7H_8	3.59	0.86
3,9-Epoxy-p-mentha-1,8(10)-diene	$C_{10}H_{14}O$	22.2	2.7
1,4-dihydroxy-p-menth-2-ene	$C_{10}H_{18}O_2$	22.347	1.29
2(3H)-Furanone,5-hexyldihydro-	$C_{10}H_{18}O_2$	27.6	6.2
Phenol, 3,5-dimethoxy	$C_8H_{10}O_3$	28.45	5.43
Diethyl Phthalate	$C_{12}H_{14}O_4$	31.08	8.31
Phenol,2,6-dimethoxy-4-(2-propenyl)-	$C_{11}H_{14}O_3$	31.38	1.55
5-Bromoadamantan-2-one	$C_{10}H_{13}BrO$	34.13	2.52
Hexanedioic acid,mono(2-ethylhexyl)ester	$C_{14}H_{26}O_4$	38.39	3.24
Cholestan-3-ol,2-methylene-, (3á,5à)-m	$C_{28}H_{48}O$	39.76	0.77
n-Hexadecanoic acid	$C_{16}H_{32}O_2$	40.73	2.34
Hexadecanoic acid, ethyl ester	$C_{18}H_{36}O_2$	40.85	1.86

Heneicosane	$C_{21}H_{44}$	41.38	2.52
Doconexent	$C_{22}H_{32}O_2$	41.85	1.08
Methanesulfonic acid,4-oxoadamantan-2-yl ester	$C_{11}H_{16}O_4S$	42.57	8.75
Methyl 4-(prop-1-en-2-yl)cyclohex-1-enecarboxylate	$C_{11}H_{16}O_2$	42.67	3.8
1-Heptatriacotanol	$C_{37}H_{76}O$	43.49	1.1
Diisooctyl phthalate	$C_{24}H_{38}O_4$	44.07	17.22
9,12,15-Octadecatrienoic acid, 2,3-dihydroxypropyl ester, (Z,Z,Z)-	$C_{21}H_{36}O_4$	44.41	1.25
Bicyclo[4.4.0]dec-2-ene-4 -ol,2-methyl-9-(prop-1-en-3-ol-2-yl)-	$C_{15}H_{24}O_2$	44.83	16.43

3.2. Concentration effect

The measurement of weight loss of mild steel in 1.0 M HCl in the absence and presence of different inhibitor concentrations was determined after 6h immersion at 298 K. The calculated values of W_{corr} and the inhibition efficiency (IE_{WL}%) are given in Table 2.

Table 2. Corrosion rate and inhibition efficiency of mild steel exposed for 6h in 1.0 M HCl at different concentrations of *Taxus baccata* (L.) extract at 298 K.

Medium	**Concentration ($g.L^{-1}$)**	**W_{corr} ($mg.cm^{-2}.h^{-1}$)**	**IE_{WL} (%)**
1.0 M HCl	---	0.6705	**---**
***Taxus baccata* (L.) extract**	0.25	0.0845	***87***
	0.5	0.0445	***93***
	0.75	0.0238	***96***
	1.0	0.0115	***98***

As can be seen in Table 2, the variation of the inhibition efficiency is in opposite trend to the corrosion rate. Indeed, the increase in the inhibition efficiency is obtained from the addition of fairly low concentrations of inhibitor and reaches the highest value at 98% at a concentration of 1.0 $g.L^{-1}$. The corrosion inhibition can be attributed to the adsorption of the molecules at the steel/HCl solution interface **[28]**.

3.3. Potentiodynamic polarization study

Figure 2 shows representative potentiodynamic polarization curves for mild steel in 1.0 M HCl solution in the absence and presence of various concentrations of *Taxus baccata* (L.) leaves extract. Using the Tafel linear extrapolation technique, values of the corrosion current density,

i_{corr}, corrosion potential, E_{corr}, and Tafel cathodic slope, β_c are determined and reported in Table 3.

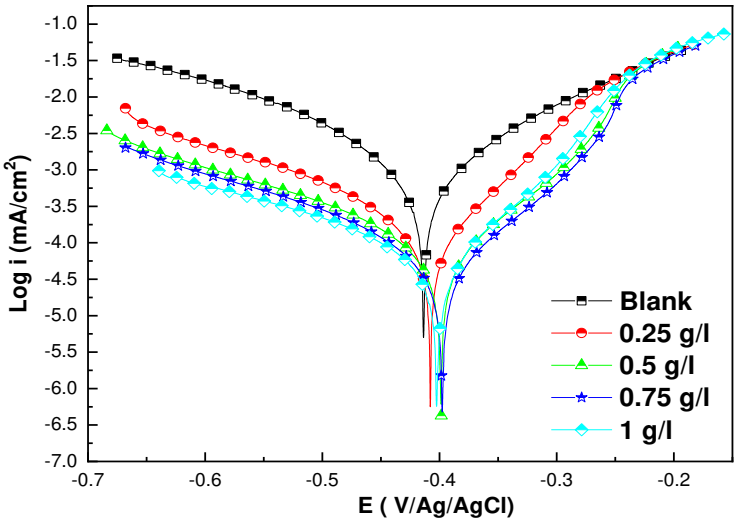

Fig. 2 Measured polarization curve for mild steel in 1.0 M hydrochloric acid in the absence and presence of different concentrations of *Taxus baccata* (L.) leaves extract

It can be seen from Fig. 9 that only the cathodic part displays a wide range of linearity, which reveals that Tafel's law is well verified in the cathodic part and the hydrogen reduction is controlled by pure activation kinetics **[29]**. It is clear from Table 3 that the increase in inhibitor concentration caused the anodic and cathodic branches to shift to lower current densities. This indicates that *Taxus baccata* (L.) leaves extract acted as a mixed type inhibitor. The results show that in the presence of *Taxus baccata* (L.) leaves extract, the cathodic Tafel slope decreased non-significantly. In addition, the decrease in the cathodic surface area can be explained by the reduction of hydrogen evolution without influencing the reaction mechanism **[30]**.

Table 3. Polarization parameters in the absence and presence of different concentrations of *Taxus baccata* (L.) leaves extract

Medium	Concentration (g/l)	$-E_{corr}$ (mV/Ag/AgCl)	i_{corr} (μA cm^{-2})	$-\beta_c$ (mV dec^{-1})	η_{PP} (%)
Blank	--	498	983	140	**---**
***Taxus baccata* (L.) extract**	0.25	408	138	158	***85***
	0.5	398	53	125	***95***
	0.75	389	43	145	***96***
	1.0	402	37	115	***96***

3.4. Electrochemical impedance spectroscopy

Figure 3 shows representative Nyquist plots of mild steel in 1.0 M HCl solution in the absence and presence of various concentrations of *Taxus baccata* (L.) leaves extract. As shown in Figure 3, it can be observed that the diameter of the capacitive loop in the pre-presence of the inhibitors is larger than in the uninhibited solution and increases with increasing inhibitor concentration. Thus, these capacitive loops are not complete half circles, which can be explained by the frequency dispersion effect resulting from the inhomogeneity of the steel surface **[31,32]**.

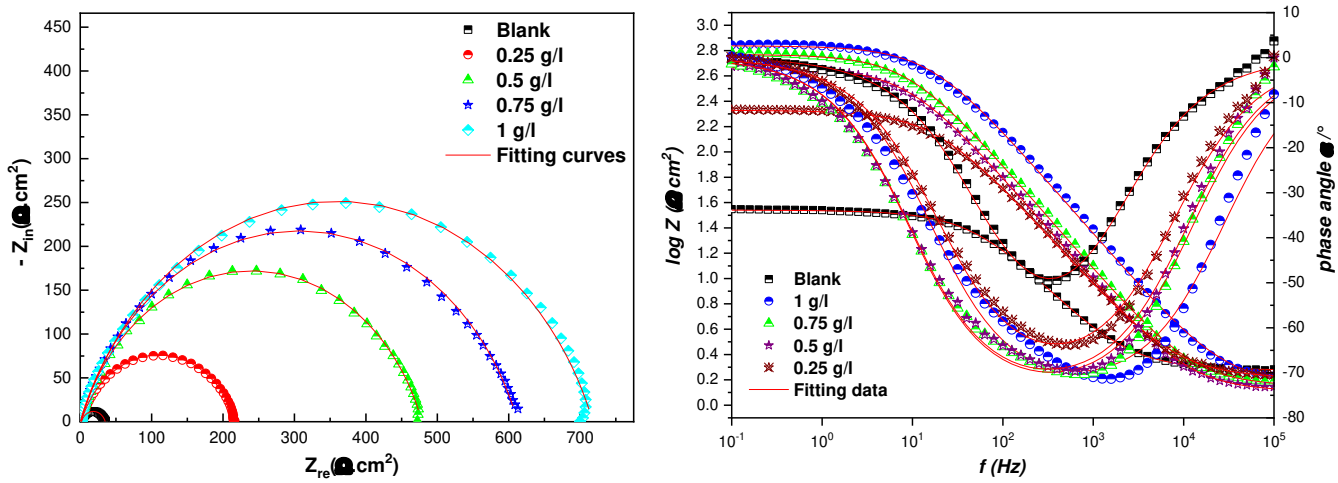

Fig.3 Nyquist diagram for mild steel in 1.0 M HCl in the absence and presence of different concentrations of the methanolic extract of *Taxus baccata* (L.)

The parameters associated with the diagram impedance such as charge transfer resistance R_{ct}, double layer capacitance C_{dl} and inhibition efficiency are presented in Table 4, after a good simulation by EC-Lab V10.02 software. From the impedance data (Table 4), it can be seen that the value of R_{ct} increases with increasing inhibitor concentration, which also indicates an increase in corrosion inhibition efficiency, reaching a maximum value of 95% at the concentration of 1.0 g/L. It can also be seen that the C_{dl} and Q values decrease with increasing inhibition efficiency, which can be explained by the adsorption of the inhibitor on the steel surface.

Table 4. Electrochemical impedance parameters in the absence and presence of different concentrations of *Taxus baccata* (L.) leaves extract

	Conc. ***(g/l)***	***R_s*** ***(Ω cm²)***	***R_{ct}*** ***(Ω cm²)***	***C_{dl}*** ***(μF.cm⁻²)***	***CPE_{dl}***		***Θ***	***η_{imp}*** ***(%)***
					n_{dl}	***Q*** ***(μF.S^{n-1})***		
Blank	--	1.76	33.2	89.10	0.784	312.7	---	**---**

Taxus	0.25	1.38	216.3	41.61	0.782	116.2	0.846	***84***
***baccata* (L.)**	0.50	0.67	477.8	40.26	0.794	90.5	0.930	***93***
extract	0.75	0.02	612.6	32.62	0.787	75.0	0.945	***94***
	1.0	0.82	717.0	16.34	0.779	43.6	0.953	***95***

3.5. Adsorption isotherm

To find information on the adsorption mechanism of *Taxus baccata* (L.) leaves extract on the surface of mild steel, it is necessary to examine the different isotherm models. For this reason, the experimental results of impedance measurements were tested with different adsorption isotherms: Langmuir, El-Awady, Temkin and Freundlich. The data obtained from the Langmuir isotherm are compatible with the examined inhibitor as they show a more appropriate value of the regression coefficient compared to the other plotted models. The linear equations for the different isotherms used are as follows (Eqs. 11-14):

Langmuir: $$\frac{C_{inh}}{\theta} = \frac{1}{K} + C_{inh} \quad (11)$$

El-Awady: $$\ln\left(\frac{\theta}{1-\theta}\right) = y \ln K + y \ln C_{inh} \quad (12)$$

Temkin: $$\theta = \frac{-1}{2a}\ln(K) - \frac{1}{2a}\ln(C_{inh}) \quad (13)$$

Freundlich: $$\ln\theta = \ln K + z \ln C_{inh} \quad (14)$$

The results obtained are presented in Fig. 4, to explore the type of adsorption of *Taxus baccata* (L.) leaves extract on mild steel, we used the Eq. (15):

$$\Delta G^{\circ}_{ads} = -RT \ln(1000 \times K_{ads}) \quad (15)$$

The calculated values of ΔG°_{ads} are inserted in Table 5.

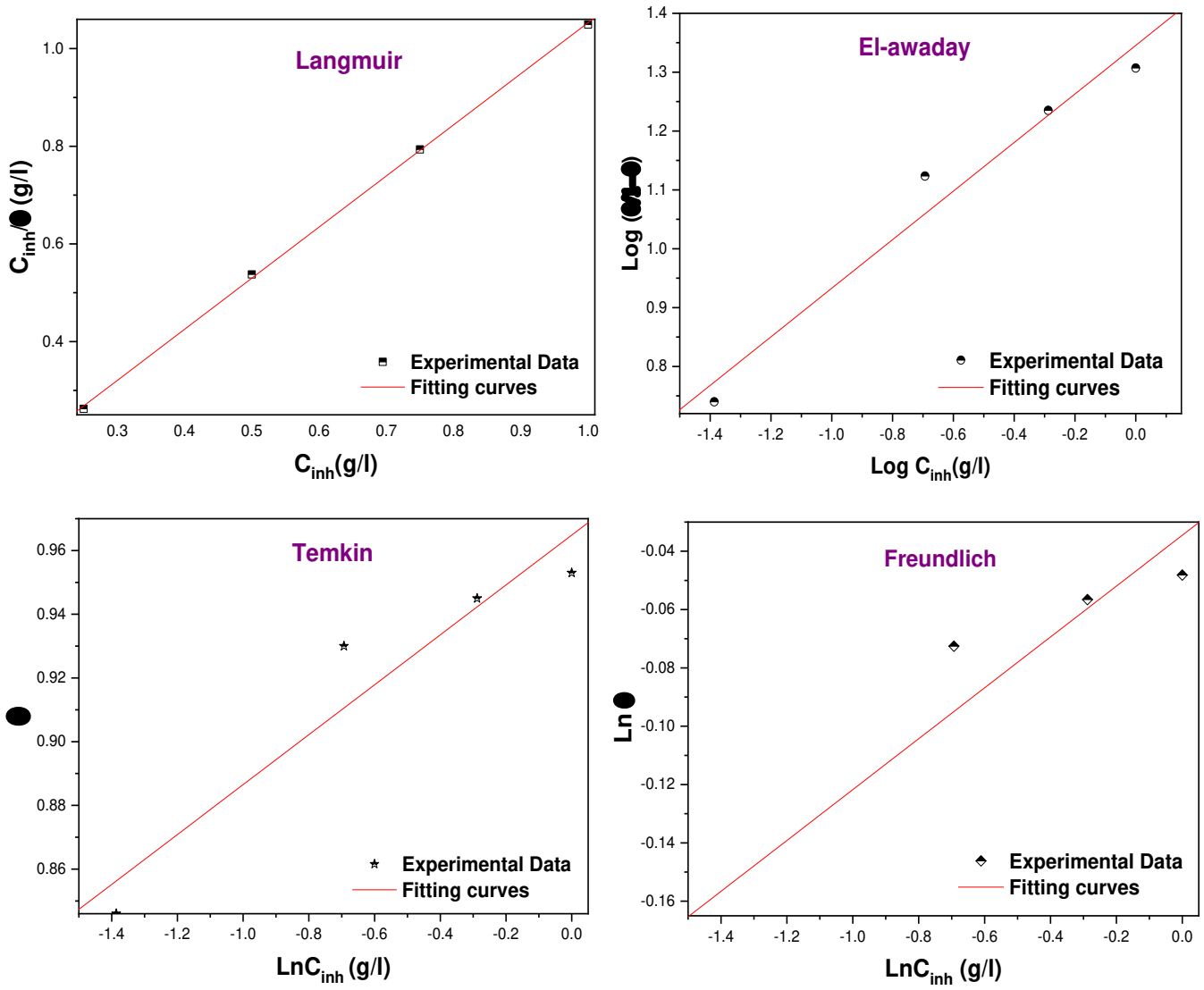

Fig. 4 Plots of *Taxus baccata* (L.) adsorption isotherm models for a mild steel surface in 1.0 M HCl at 298 K obtained from the EIS data

Generally, when $\Delta G°_{ads}$ is about -20 Kj.mol^{-1}, or less negative, the interactions between the charged mild steel surface and the charged extract compounds are electrostatic and the adsorption is physical. Whereas, when the values of $\Delta G°_{ads}$ are close to -40 kJ-mol^{-1} or more negative, in this case, there is electron transfer from the inhibitor molecules to the metal surface and the adsorption is chemical **[33,34]**. According to the results obtained, the type of adsorption of *Taxus baccata* (L.) leaves extract is physisorption.

Table 5. Adsorption parameters deduced from different adsorption isotherms of Taxus baccata (L.) leaves extract at 298 K

Isotherms	***R^2***	***Parameter***	***K_{ads} $(L.g^{-1})$***	***ΔG^0_{ads} $(KJ.mol^{-1})$***

Langmuir	0.999	slope	1.046	154.08	-29.61
El-Awady	0.982	1/y	2.423	1.74	-18.50
Temkin	0.955	a	-6.384	12.31	-23.35
Freundlich	0.952	a	0.087	0.96	-16.95

3.6. Immersion time

The evolution of the inhibition process as a function of immersion time provides interesting information on the stability of the inhibitor film, and we carried out electrochemical impedance spectroscopy measurements in a 1.0 M HCl solution in the absence and presence of the inhibitor for immersion times of 1h to 12 h at 298K. The results are shown in Figure 5 and Table 6.

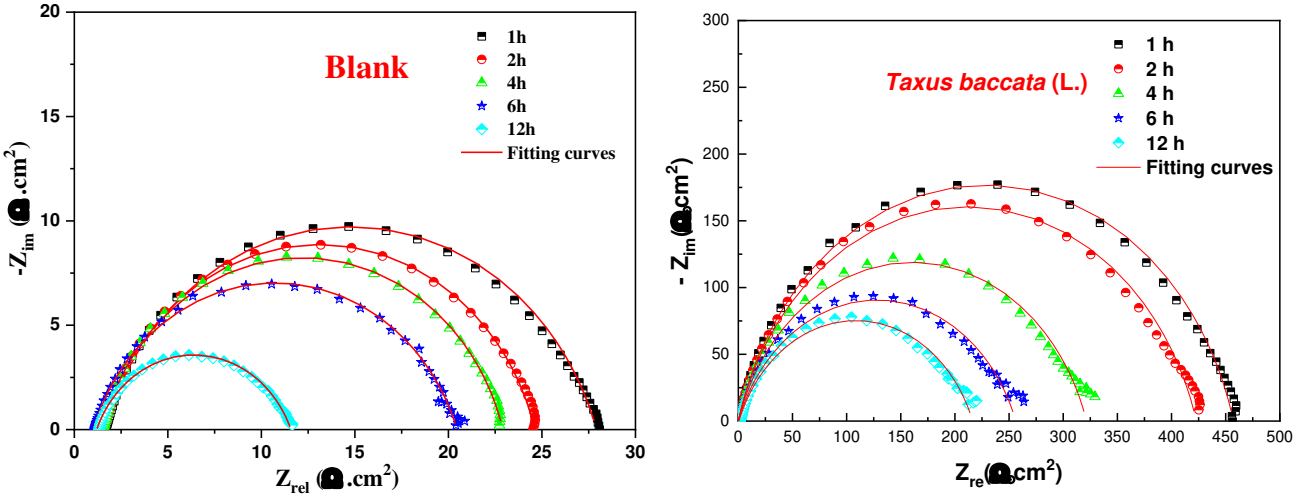

Fig.5 Impedance spectra obtained after different immersion times in a 1.0 M HCl solution without (a) and with (b) 1.0 g/L *Taxus baccata* (L.) leaves extract

It is clear from these results that the charge transfer resistance R_{ct} increases after 1 h of immersion in the inhibitor and then it starts to decrease. On the other hand, the optimal value of inhibition efficiency obtained after 1 h of immersion reaches 90% but after 12 hours the percentage of efficiency decreases to a value of 85%. These results can be explained by the formation of the tested extract molecules of a resistance film with time in 1h **[35]**. However, after a longer immersion time, the protective film formed on the surface of the mild steel dissolved **[36]**.

Table 6. Impedance parameters of mild steel in the absence and presence of 1.0 g/L *Taxus baccata* (L.) leaves extract at different immersion periods

Medium	*Time (h)*	*Rs* ($\Omega.cm^2$)	*Q* ($\mu F.Sn^{-1}$)	R_{ct} ($\Omega.cm^2$)	CPE_{dl}		*IE (%)*
					n_{dl}	C_{dl} ($\mu F.cm^{-2}$)	
Blank	1	0.358	--	42.9	--	331	--
	2	1.097	--	41.9	--	333	--
	4	356	--	40.9	--	348	--
	6	0.359	--	36.9	--	408	--
	12	0.364	--	30.6	--	724	--
***Taxus baccata* (L.) extract**	1	0.101	53	457.0	0.838	26	***90.5***
	2	0.17	63	423.1	0.826	29	***90.0***
	4	0.149	106	321.7	0.81	48	***87.2***
	6	0.019	162	256.2	0.784	67	***85.5***
	12	0.58	202	215.8	0.775	81	***85.8***

3.7. Temperature effect

To study the effect of temperature on the inhibition efficiency of *Taxus baccata* (L.) leaves extract, experiments were conducted in the range of 298 to 328 K using weight loss measurements at 2 h. The corrosion parameters obtained are presented in Table 7.

Table 7. Corrosion parameters obtained from weight loss for mild steel in 1.0 M HCl containing 1.0 g/L *Taxus baccata* (L.) leaves extract at different temperatures

Inhibitor	Temperature (K)	C_R ($mg.cm^{-2}.h^{-1}$)	IE %
Blank	398	0,8625	--
	308	1,1512	--
	318	1,4656	--
	328	2,3318	--
***Taxus baccata(L.)* extract**	398	0,0446	***94***
	308	0,0943	***92***
	318	0,1540	***89***
	328	0,3214	***86***

The results in Table 7 show a remarkable decrease in inhibition efficiency when increasing the temperature in the presence of inhibitor. The thermodynamic activation parameters were calculated from the effect of the temperature result obtained by polarization curves. The

apparent activation energy E_a, activation enthalpy ΔH^* and activation entropy ΔS^* were extracted using the Arrhenius equations Eqs. (16) and (17) **[37]**.

$$i_{corr} = A e^{\left(\frac{-E_a}{RT}\right)} \qquad (16)$$

$$i_{corr} = \frac{RT}{Nh} \; e^{\left(\frac{\Delta S^*}{R}\right)} \; e^{\left(\frac{-\Delta H^*}{RT}\right)} \qquad (17)$$

Where A is the Arrhenius pre-exponential constant, E_a is the apparent activation energy, R is the gas constant, T is the absolute temperature, h is Plank's constant, N is the Avogadro number. Arrhenius plots for the corrosion rate of mild steel are given in Figure 6. The values of E_a, ΔH^* and ΔS^* are given in Table 8.

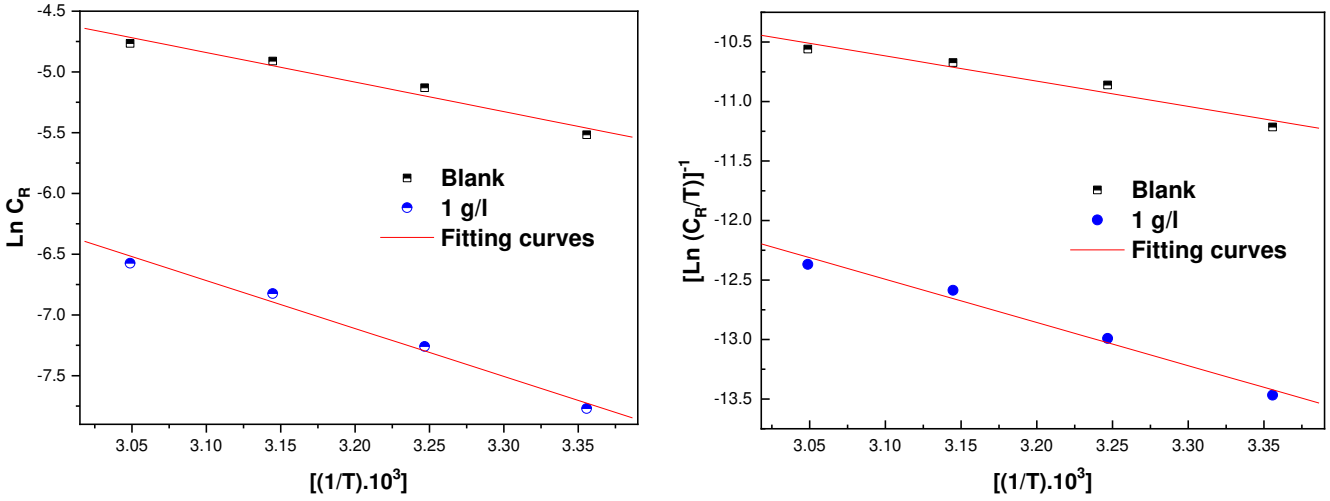

Fig. 6 Arrhenius curves Ln C_R and Ln (C_R/T) vs. 1000/T in 1.0 M HCl with and without 1.0 g/L of *Taxus baccata* (L.)

It can be seen that the activation energy increases in the presence of an inhibitor. Generally, the higher E_a value indicates a strong inhibitory action by increasing the energy barrier for the corrosion process, highlighting the electrostatic character of the inhibitor adsorption on the mild steel surface **[38]**. Moreover, the value of E_a which is around 40-80 KJ.mol-1 can be suggested to obey the physical adsorption mechanism (physisorption). Furthermore, the value of ΔH^* for the dissolution reaction of mild steel in 1.0 M HCl solution in the presence of the inhibitor are higher than in their absence, the positive sign of ΔH^* shows that the dissolution reaction is endothermic. In addition, it can be noted that the high negative value of ΔS^* in the presence of *Taxus baccata* (L.) extract indicates a decrease in disorder during the formation of the metal/adsorbate complex compound **[39]**.

Table 8. Activation parameters E_a, ΔH^* and ΔS^* of the dissolution of mild steel in 1.0 M HCl solution in the absence and presence of 1.0 g/l *Taxus baccata* (L.) leaves extract

Activation parameter	***Blank***	***Taxus baccata (L.) extract***
E_a (kJ.mol^{-1})	26.9	53.83
ΔH^* (kJ.mol^{-1})	24.3	51.19
ΔS^*(J.mol^{-1}.K^{-1})	-178.3	-113.98

3.8. Scanning electron microscopy (SEM)/EDX

The morphological characteristics of mild steel before and after immersion in 1.0 M hydrochloric acid for 6 hours in the absence and presence of 1g/l of *Taxus baccata* (L.) leaves extract is presented in Figure 7. The composition of the mild steel before and after treatment is shown in Figure 8 and Table 9.

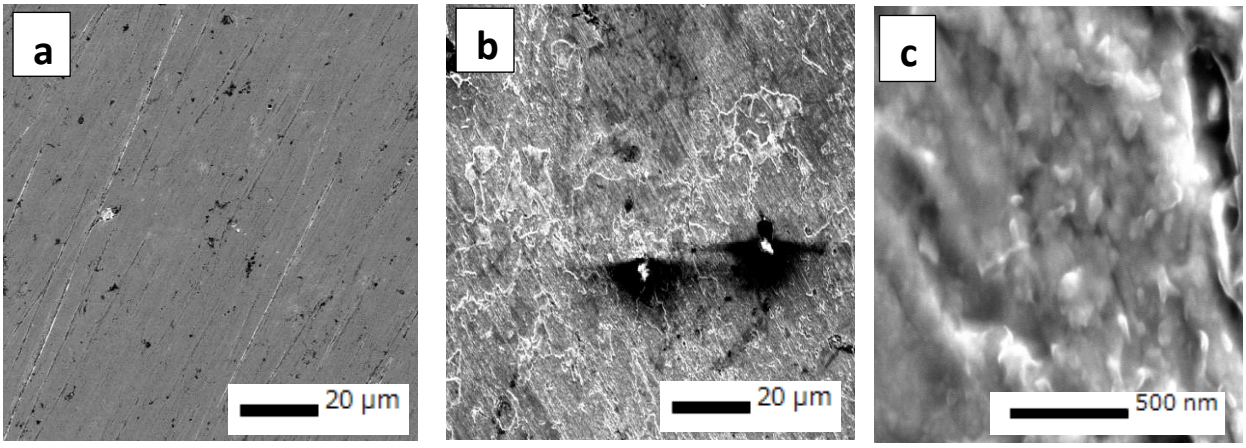

Fig. 7 SEM image of the mild steel surface (a) before and (b) after 6 hours immersion in 1.0 M HCl solution in the absence of inhibitors and (c) after 6 hours immersion in 1.0 M HCl solution in the presence of 1.0 g/l inhibitor.

It can be seen from this figure that the steel sample without inhibitor (b) is heavily corroded by the appearance of grey clusters and some pitting due to the aggressive solution. In the presence of inhibitor (c), the steel surface is almost free of corrosion. This is due to the formation of an adsorbed layer of the extract on the surface. These observations show that the examined extract prevents corrosion of mild steel by limiting the access of the electrolyte to the surface.

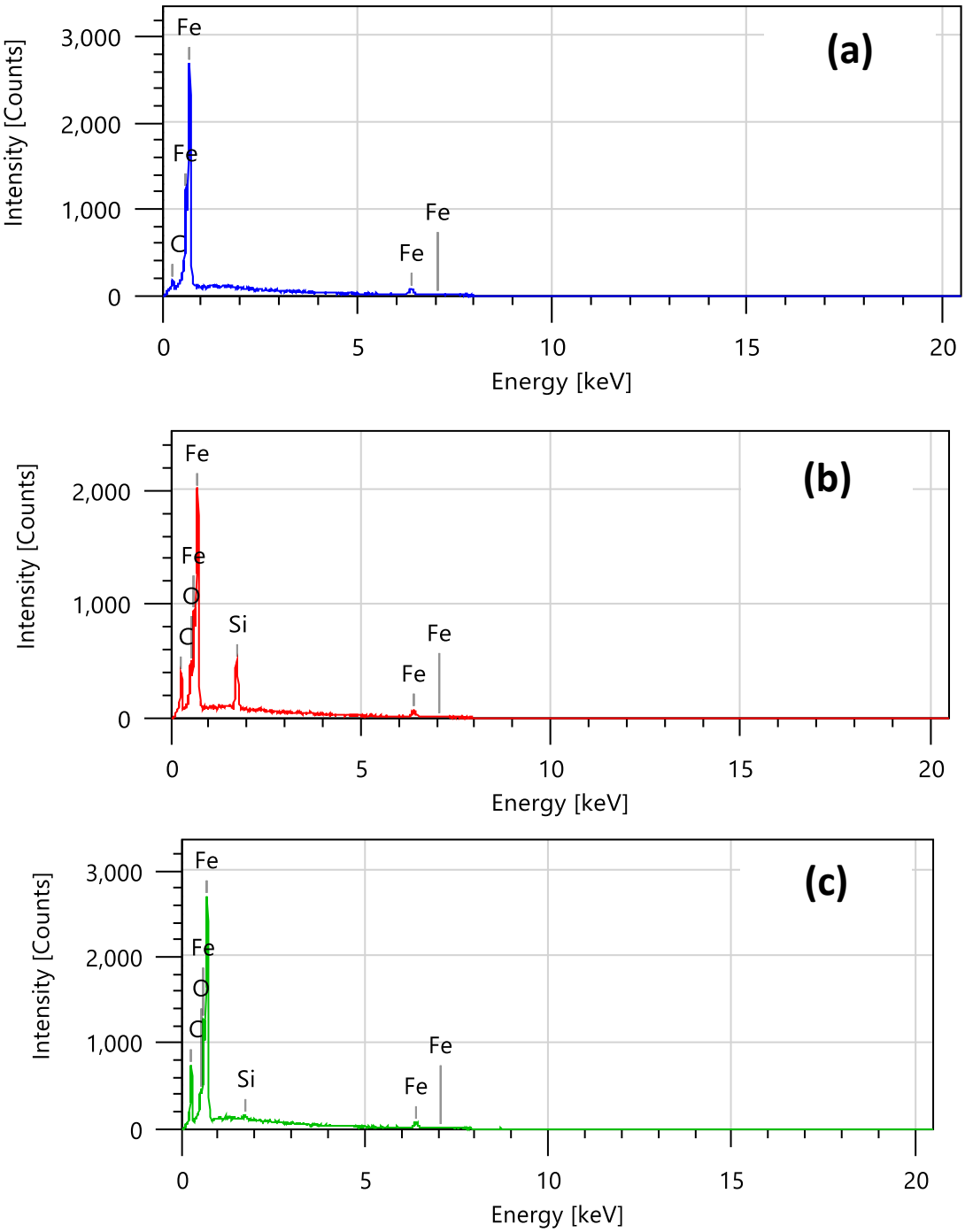

Fig. 8. EDX spectra of mild steel before immersion (a), after 6 h immersion in 1.0 M HCl (b), after immersion in 1.0 g/l *Taxus baccata* (L.) leaves extract

Figure 8 shows the general EDX spectrum made on the mild steel surface before immersion (a), after 6 hours immersion in 1.0 M HCl at 25 °C (b) and after immersion in 1.0 M HCl+1.0 g/l *Taxus baccata* (L.) leaves extract (C). The comparison of the spectra (a) and (b) shows well First, the atomic percentage of iron decreases from 98.52% to 85.74% (Table 9) and the increase of carbon percentage after immersion in 1.0 M HCl. Then the formation of iron oxide from the corrosion of the steel, as shown by the appearance of the oxygen peak on the EDX spectrum

(b) with an atomic percentage of (3.19 %). The presence of the silicon peak, indicating the presence of this element on the surface, can also be seen after 3 hours of immersion. The comparison of the two EDX spectra (a) and (b) with the EDX spectrum (c), clearly shows that the silicon and oxygen peak decreases strongly on the EDX spectra of the extract. These observations confirm that the extract seems to stop corrosion of the steel by forming a layer that limits the access of the electrolyte to the surface **[40]**. Finally, these results confirmed the inhibition efficiency obtained experimentally.

Table 9. The weight percentage of elements obtained from EDX spectra

Inhibitors	Fe	C	O	Si
Mild steel	98.52	1.48	**	**
Mild steel+1.0 M HCl	85.74	4.96	3.19	6.12
Mild steel + *Taxus baccata* (L.)	88.67	8.46	2.34	0.52

3.9. Computational investigation

It was shown that the inhibitive activity of a molecule is influenced by its electronic structure as well as by its molecular geometry. In this present work, the DFT method was utilized with B3LYP-6-311G (d,p) basis set in the aqueous phase. Fig. 9 displays the optimized molecular configurations, the electronic distribution of HOMO and LUMO molecular orbitals as well as the electrostatic potential (ESP) of A, B, C and D in the aqueous medium. The distribution of HOMO and LUMO orbitals in inhibitory molecules can be described as having a significant role in the prediction of the potential to give and receive electrons from/to metal surfaces, respectively. From Fig. 9, It was found that the HOMO electron density of A and B are located on the methyl-propenol group and dimethyl phthalate ring. In addition, it was distributed on almost the whole molecule for C and D molecules. For LUMO orbitals, it can be observed that C and D are distributed almost over the molecular structures. This points out that the exchange of electrons from HOMO to LUMO (from/to the vacant metal orbits of the steel surface) with the formation of a bond between the investigated reactants is easy **[41]**.

OPT-structure

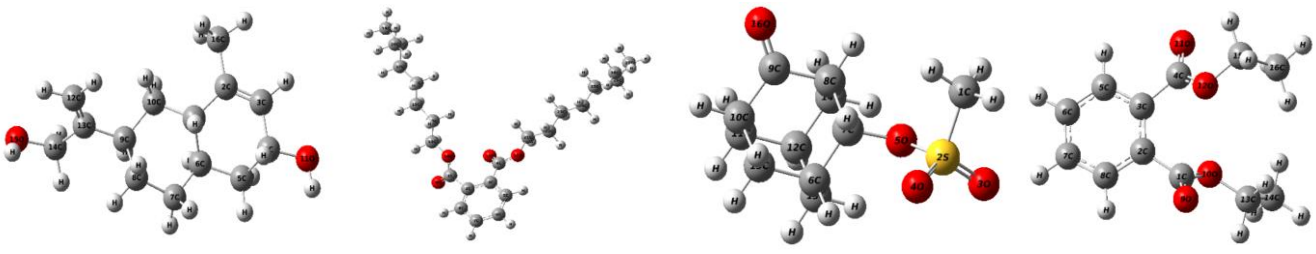

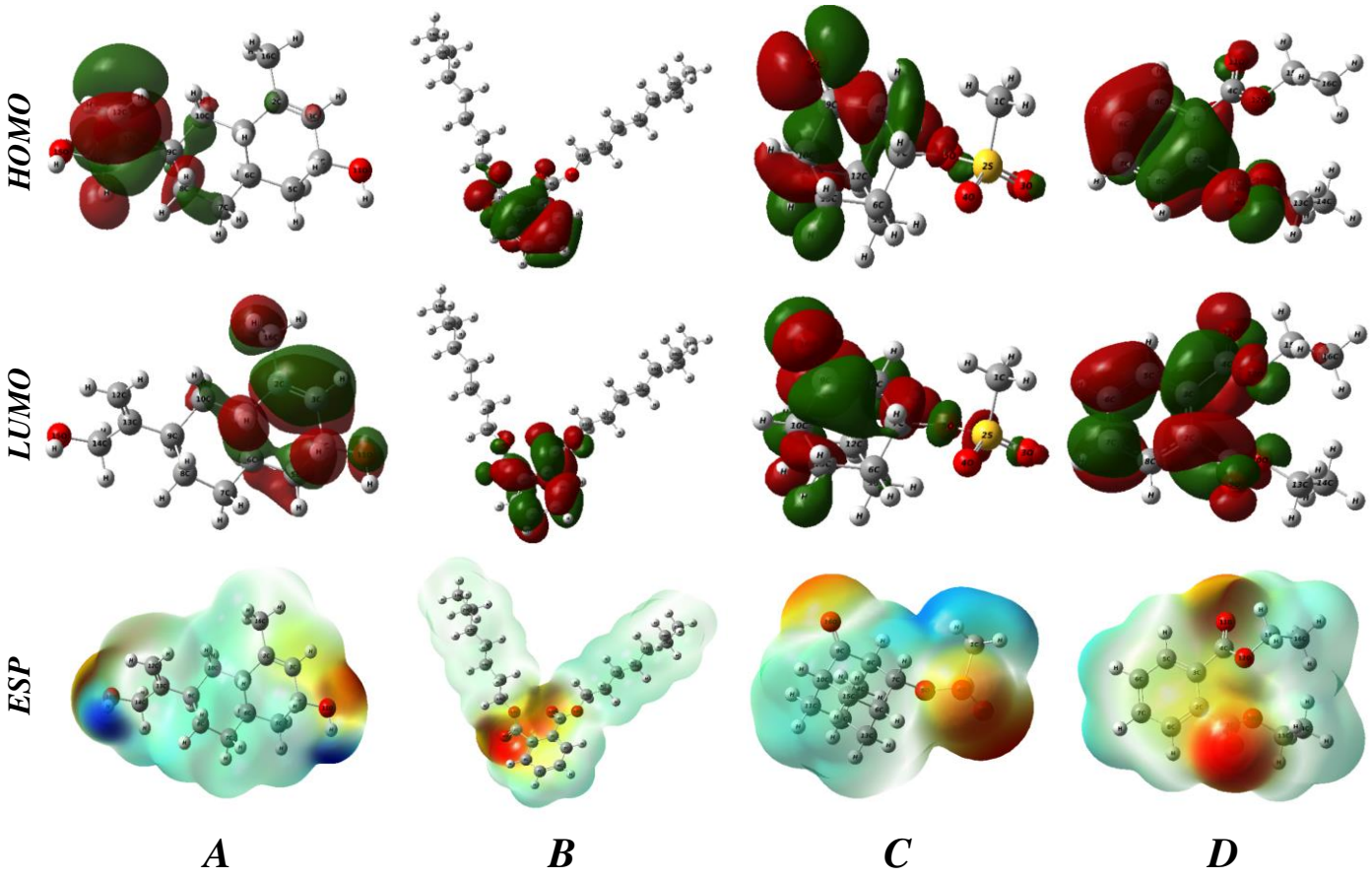

Fig.9. Optimized structure, Frontiers orbitals (HOMO and LUMO) and ESP maps of major molecules in *Taxus baccata (L.)*

Table 10. DFT descriptors for A, B, C and D in aqueous phase.

Quantum chemical descriptor	***A***	***B***	***C***	***D***
E_{HOMO}**/eV**	-6,429	-7,370	-6,907	-7,392
E_{LUMO}**/eV**	0,280	-1,781	-0,871	-1,770
ΔE_g**/eV**	6,710	5,589	6,036	5,621
Electronegativity $\chi = (I + A)/2$	3,074	4,575	3,889	4,581
Chemical softness $S = 1/\eta$	0,298	0,357	0,331	0,355
$\Delta E_{back\text{-}donation} = -\eta/4$	-0,838	-0,698	-0,754	-0,702
Fraction of electron transferred $\Delta N = \frac{\Phi - \chi_{inh}}{2(\eta_{Al} + \eta_{inh})}$ **For Al** Φ**=4.82 eV,** $\eta_{Al} = 0$	0,260	0,0437	0,154	0,042

Generally, a high E_{HOMO} values reflect a high tendency to donate electrons **[42]**. However, the high electron acceptance capacity is linked with a small E_{LUMO} value **[43]**. From the collected

data in Table 10 of all considered molecules, it can be observed that the E_{HOMO} of B and D is higher than that of A and C. This implies that these molecular species have a higher tendency to donate their electrons to the steel surface. The same result has been found from the computed gap energies, which reflect its maximum global reactivity compared to the A and C molecules. The order of their energy gap values is B (5.589 eV) < D (5.621 eV) < C (6.036 eV) < A (6.710 eV). In addition, it is seen from Table 10, that the high potential of B and D is confirmed by the smaller values of the chemical softness (S), this order is effectively correlated with the previous conclusions. Using Lukovits' investigation, which demonstrated that a positive value of the transferred electron number $\Delta N < 3.6$, the ability to cede electrons to the metal surface enhances the inhibition ability of a molecule **[44,45]**. In this work, all studied molecules have values of ΔN inferior to 3.6, hence the inhibitor molecules act as electron donors. It can be indicated that all determined descriptors can be involved in the inhibitor-metal interaction in terms of the donor-acceptor process and have high chemical activity.

Nucleophilic and electrophilic attack is monitored by the maximum values of the condensed Fukui functions which are an indication of the highest reactive center of a molecule **[46]**. Table 11 represent electrophilic/nucleophilic attacks of neutral major molecules in terms of atom-condensed Fukui functions in aqueous medium. f_k^+ values represent the reactivity towards the nucleophilic attack and f_k^- values represent the reactivity towards the electrophilic attack when the molecule loses electrons. Based on Table 12. the favored sites for the nucleophilic attack in the P1 inhibitor are the O11, O15, C2 and C12 atoms. While the favored sites for the electrophilic agent are C3, C2, O11 and C12 atoms. For the molecule P2. the most reactive sites for electrophilic attack are oxygen atoms. On the other hand. C6. C2. N3 and O9 are the most susceptible sites for nucleophilic attacks. In addition. the results of Table 12 indicated that heteroatoms such as oxygen and sulfur atoms in P3 molecules are suitable sites for both nucleophilic and electrophilic attacks. Furthermore. the most reactive sites for electrophilic and nucleophilic attacks are C3. C6. C7. O9 and O11.

Table 11 Fukui functions of P1, P2, P3 and P4 computed using B3LYP/6-31G(d,p) in aqueous phase

Inhibitor	*Atom k*	*P(N-1)*	*P(N)*	*P(N+1)*	f_k^+	f_k^-
P1	**O15**	8.879	8.779	8.776	0.099	0.00236
	O11	8.866	8.789	8.744	0.076	0.045
	C2	6.049	5.975	5.733	0.074	0.241

	C12	6.484	6.420	6.379	0.064	0.040
	C3	6.286	6.245	5.969	0.040	0.275
	C13	6.051	6.015	5.994	0.036	0.021
P2	**C6**	6.300	6.179	6.158	0.121	0.020
	C2	6.243	6.130	6.124	0.112	0.006
	C3	6.229	6.128	6.139	0.100	-0.010
	O9	8.735	8.643	8.549	0.091	0.094
	O11	8.633	8.563	8.311	0.070	0.251
	O10	8.531	8.503	8.344	0.028	0.159
	O12	8.603	8.574	8.483	0.029	0.091
	C4	5.255	5.199	5.136	0.091	0.094
P3	**C9**	5.591	5.371	5.381	0.219	-0.009
	O16	8.734	8.589	8.562	0.144	0.027
	S2	13.849	13.743	13.736	0.106	0.006
	O5	8.769	8.702	8.655	0.067	0.046
	O3	8.982	8.926	8.853	0.055	0.073
	O4	8.949	8.912	8.720	0.037	0.192
	C13	6.401	6.401	6.283	0.0002	0.117
P4	**C7**	6.328	6.186	6.066	0.142	0.120
	C3	6.233	6.126	6.021	0.107	0.104
	C6	6.293	6.189	6.080	0.103	0.109
	C2	6.221	6.121	6.025	0.100	0.096
	O11	8.697	8.607	8.442	0.089	0.164
	O9	8.668	8.605	8.458	0.063	0.146

Conclusion

Corrosion inhibition performance of *Taxus baccata* (L.) leaves extract on mild steel was investigated in 1.0 M HCl solution by using weight loss, potentiodynamic polarization (PP), electrochemical impedance spectroscopy (EIS), scanning electron microscope (SEM) coupled with EDX analysis. the weight loss study displays that a decrease in the corrosion rate with an inhibitory efficiency is of the order of 98% at 1.0 g/l of *Taxus baccata* (L.) leaves extract. Besides, the EIS measurements have better inhibitory efficiency of 95% for 1.0 g/l of *Taxus baccata* (L.) leaves extract. The PP results indicated a mixed-type character of studied extract as they adsorb on the steel surface following the Langmuir model. Further surface film

formation is confirmed by SEM and EDX analysis. DFT calculations revealed that both examined molecules could act as electron donor/acceptor to/from the steel surface.

Acknowledgments the Director of Molecular Chemistry and Natural Substance, Moulay Ismail University, Faculty of Science, Meknes and the Director of Engineering Laboratory of Organometallic, Molecular Materials, and Environment, Faculty of Sciences, University Sidi Mohamed Ben Abdellah, Fez. Morocco.

Funding Not applicable.

Data Availability The data used during the study appear in the submitted article.

Declarations

Conflict of interest The authors declare no conflict of interest.

Data Availability Statements All data generated or analysed during this study are included in this published article (and its supplementary information files).

References

[1] Chauhan DS, Ansari KR, Sorour AA, Quraishi MA, Lgaz H, Salghi R (2018) Thiosemicarbazide and thiocarbohydrazide functionalized chitosan as ecofriendly corrosion inhibitors for carbon steel in hydrochloric acid solution. Int. J. Biol. Macromol 107 :1747–1757.

[2] Haque J, Srivastava V, Verma C, Lgaz H, Salghi R, Quraishi MA (2017) N-Methyl-N, N, N-trioctylammonium chloride as a novel and green corrosion inhibitor for mild steel in an acid chloride medium: electrochemical, DFT and MD studies, New J. Chem. 41 (22) 13647-13662.

[3] Gupta NK, Verma C, Salghi R, Lgaz H, Mukherjee AK, Quraishi MA (2017) New phosphonate based corrosion inhibitors for mild steel in hydrochloric acid useful for industrial pickling processes: experimental and theoretical approach, New J. Chem, 41(21) 13114–13129,

[4] Ostovari A, Hoseinieh SM, Peikari M, Shadizadeh SR, Hashemi SJ (2009) Corrosion inhibition of mild steel in 1 M HCl solution by henna extract: A comparative study of the inhibition by henna and its constituents (Lawsone, Gallic acid, α-D-Glucose and Tannic acid), Corros. Sci, 51(9) 1935–1949.

[5] Abiola OK, Tobun Y, (2010) Cocos nucifera L. water as green corrosion inhibitor for acid corrosion of aluminium in HCl solution, Chinese Chem. Lett, 21(12) 1449–1452.

[6] Thomas PA, Polwart A, (2003) Taxus baccata, no. McEvoy 1943 489–524.

[7] Kucukboyaci N, Sener B, Choudhary M (2004) Bioactivity of Lignans from Taxus baccata, *Z.* Naturforsch. *C.*, 59 494–498

[8] Krauze-Baranowska M, Wiwart M (2003) Antifungal activity of biflavones from Taxus baccata and Ginkgo biloba, *Z.* Naturforsch. C, 58 65–69.

[9] Kucukboyac N, Orhan I, Şener B, Nawaz SA, Choudhary MI (2010) Assessment of Enzyme Inhibitory and Antioxidant Activities of Lignans from Taxus baccata L.," Zeitschrift für Naturforsch. C, 65 187–194.

[10] Emami SA, Sadeghi-aliabadi H, Saeidi M, Jafarian (2005) A Cytotoxic Evaluations of Iranian Conifers on Cancer Cells, Pharm. Biol, 43 (4) 299–304.

[11] Kucukboyaci N, Sener B (2010) Biological activities of lignans from Taxus baccata L. growing in Turkey, Journal de recherche sur les plantes médicinales 4 (12) 1136–1140.

[12] Riffi O, Amechrouq A, Elhourri M, El Idrissi M, Fliou J (2019) study of the insecticidal activity of taxus baccata of the ifrane valley on sitophilus oryzae (l.) (coleoptera: curculionidae), Bulletin environnemental Fresenius, 28(4) 3197–3202.

[13] Bajić V, Stanimirović Z, Stevanović J, Milićević Z, Živković L, Potparević B (2010) The effect of paclitaxel alone and in combination with cycloheximide, Arch. Biol. Sci., Belgrade 62(1) 63-74.

[14] Asghari G, Mostafavi SA, Esmaeili A (2009) Solvent optimization on Taxol extraction from Taxus baccata L, using HPLC and LC-MS. DARU, 17(3) 192–198.

[15] Lal M, Borah A, Pandey SK (2019) Identification of a New High Geraniol Rich Variety 'Jor Lab L-15' of Lemongrass [Cymbopogon khasianus (Hack) Stapf (ex Bor)], J. Essent. Oil Bear. Plants, 22(4) 972–978.

[16] Lal M, Dutta S, Munda S, Pandey SK (2018) Identification and Registration of a High Essential Oil Yielding Variety (Jor Lab L-14) of Lemongrass (Cymbopogon flexuosus L.) Through Mutation Breeding Technique, J. Essent. Oil Bear. Plants, 21(6) 1604–1611

[17] Nahlé A, Salim R, El Hajjaji F, Aouad MR, Messali M, Hammouti B, Taleb M (2021) Novel triazole derivatives as ecological corrosion & theoretical approach; RSC Advances 4147–4162.

[18] Salim R, Nahlé A, El-Hajjaji F, Ech-chihbi E, Benhiba F, El Kalai F, Benchat N, Oudda H, Guenbour A, Taleb M, Warad I, Zarrouk A, (2021) Experimental, Density Functional Theory, and Dynamic Molecular Studies of Imidazopyridine Derivatives as Corrosion Inhibitors for Mild Steel in Hydrochloric Acid, Surf. Eng. Appl. Electrochem, 57 233–254.

[19] Seeger ZL, Izgorodina EI (2020) A systematic study of DFT performance for geometry optimizations of ionic liquid clusters, J. Chem. Theory Comput., 16 (10) 6735-6753

[20] Douche D, Elmsellem H., Anouar EH, Guo L, Hafez B, Tüzün B, El Louzi A, Bougrin K, Karrouchi K, Himmi B, (2020) Anti-corrosion performance of 8-hydroxyquinoline derivatives for mild steel in acidic medium: Gravimetric, electrochemical, DFT and molecular dynamics simulation investigations, Journal of Molecular Liquids 308 113042.

[21] Salim R, Ech-chihbi E, Oudda H, El Hajjaji F, Taleb M, Jodeh S, (2019) A review on the assessment of imidazole [1,2-a] pyridines as corrosion inhibitor of metals, Journal of Bio-and Tribo-Corrosion. 13: 5–11.

[22] El Hajjaji F, Salim R, Messali M, Hammouti B, Chauhan DS, Almutairi SM, Quraishi MA (2019) Electrochemical studies on new Pyridazinium derivatives as corrosion inhibitors of carbon steel in acidic medium. Journal of Bio-and Tribo-Corrosion 5:4.

[23] Obot IB, Macdonald DD, Gasem ZM (2015) Density functional theory (DFT) as a powerful tool for designing new organic corrosion inhibitors. Part 1: an overview,

Corrosion Sci., 99 1-30

[24] El-Hajjaji F, Ech-chihbi E, Rezki N, Benhiba F, Taleb M, Chauhan DS, Quraishi MA, (2020) Aperçus électrochimiques et théoriques sur l'adsorption et l'inhibition de la corrosion de nouveaux liquides ioniques dérivés du pyridinium pour l'acier doux dans 1 M HCl. J. Mol. Liq., 314 : 113737

[25] Ouakki M, Galai M, Rbaa M, Abousalem AS, Lakhrissi B, Rifi EH, Cherkaoui M (2020) Investigation of imidazole derivatives as corrosion inhibitors for mild steel in sulfuric acidic environment: experimental and theoretical studies, Ionics, 26: 5251-5272 https://doi.org/10.1007/s11581-020-03643-0

[26] Schneider B, Zhao Y, Blitzke T, Schmitt B, Nookandeh A (1998) Taxane Analysis by High Performance Liquid Chromatography – Nuclear Magnetic Resonance Spectroscopy of Taxus Species §, 237–244

[27] Qin F, Wang S, Guo R, Zhang Y, Gu Y, Shi Q (2013) Chemical Studies on Taxus canadensis," 10: 1729–1753,.

[28] Khaled KF (2011) Studies of the corrosion inhibition of copper in sodium chloride solutions using chemical and electrochemical measurements, Mater. Chem. Phys, 125, (3) 427–433,.

[29] Aithaddou B, Chebabe D, Dermaj A, Benassaoui H, El Assyry A, Hajjaji N, Ahmed SI, Srhiri A (2016) Comparative study of low carbon steel corrosion inhibition in 1M HCl by 1,2,4-triazole-5-thione derivatives, J. Mater. Environ. Sci., 7 (6) 2191-12000

[30] Alibakhshi E, Ramezanzadeh M, Bahlakeh. Ramezanzadeh GB (2018) Glycyrrhiza glabra leaves extract as a green corrosion inhibitor for mild steel in 1 M hydrochloric acid solution: Experimental, molecular dynamics, Monte Carlo and quantum mechanics study, J. Mol. Liq., 255 185–198.

[31] Al-ghamdi AF, Messali M, Ahmed SA (2011) Electrochemical Studies of New Pyridazinium-based Ionic Liquid and its Determination in Different Detergents, J. Mater. Environ. Sci. 2 (3) 215-224

[32] Ghazoui A, (2017) The study of the effect of ethyl (6-methyl-3-oxopyridazin-2-yl) acetate on mild steel corrosion in 1M HCl, J. Alloys Compd., 693 510–517.

[33] Bentiss F, Lebrini M, Vezin H, Lagrenee M (2004) Experimental and theoretical study of 3-pyridyl-substituted 1,2,4-thiadiazole and 1,3,4-thiadiazole as corrosion inhibitors of mild steel in acidic media, Mater. Chem. Phys, (87)18.

[34] Noor EA, Al-Moubaraki AH (2008) Thermodynamic study of metal corrosion and inhibitor adsorption processes in mild steel/1-methyl-4[4′(-X)-styryl pyridinium

iodides/hydrochloric acid systems, Mater. Chem. Phys, 110(1) 145–154,

[35] Ech-chihbi E, Belghiti ME, Salim R, Oudda H, Taleb M, Benchat N, Hammouti B, El-Hajjaji F (2017) Experimental and computational studies on the inhibition performance of the organic compound '2-phenylimidazo [1,2-a] pyrimidine-3-carbaldehyde' against the corrosion of carbon steel in 1.0 M HCl solution, Surfaces and Interfaces, 9206–217.

[36] Ouakki M, Galai M, Benzekri Z, Verma C, Ech-chihbi E, kaya S, Boukhris S, Ebenso EE, Touhami ME, Cherkaoui M (2021) Insights into corrosion inhibition mechanism of mild steel in 1 M HCl solution by quinoxaline derivatives: Electrochemical, SEM/EDAX, UV-visible, FT-IR and theoretical approaches. Colloids. Surf. A Physicochem. Eng. Asp, 611 :125810

[37] Yadav M, Behera D, Kumar S (2014) Experimental and theoretical investigation on adsorption and corrosion inhibition properties of imidazopyridine derivatives on mild steel in hydrochloric acid solution, Surf. Interface Anal, 46(9) 640–652.

[38] Awad MI, (2006) Eco friendly corrosion inhibitors: Inhibitive action of quinine for corrosion of low carbon steel in 1M HCl, J. Appl. Electrochem, 36 :1163–1168

[39] Andreani S, Znini M, Paolini J, Majidi L, Hammouti B, Costa J, Muselli A (2016)Study of Corrosion Inhibition for Mild Steel in Hydrochloric Acid Solution by Limbarda crithmoides (L.) Essential Oil of Corsica, J. Mater. Environ. Sci. 7 (1) 187-195.

[40] Arrousse N, Salim R, Abdellaoui A, El Hajjaji F, Hammouti B, Mabrouk EH, Dino WA, Taleb M, (2021) Synthesis, characterization, and evaluation of xanthene derivative as highly effective, nontoxic corrosion inhibitor for mild steel immersed in 1 M HCl solution, J. Taiwan Inst. Chem. Eng, 120: 344–359

[41] Lazrak J, Ech-chihbi E, El Ibrahimi B, El Hajjaji F, Rais Z, Tachihante M, Taleb M, (2022) Detailed DFT/MD simulation, surface analysis and electrochemical computer explorations of aldehyde derivatives for mild steel in 1.0 M HCl, *Colloids. Surf. A* Physicochem. Eng. Asp, 632: 127822

[42] El kalai F, Chelfi T, Benchat N, Bouklah M, Daoui S, Karrouchi K, Allali M, Taleb M, Ech chihbi E, Almalki FA, Ben Hadda T (2020) New Heterocyclic Compounds Based on Pyridazinones Scaffold as Efficient Inhibitor of Corrosion of Mild Steel in Acidic Solution 1Â M HCl, Journal of Bio- and Tribo-Corrosion 6: 89.

[43] Ouakki M, Galai M, Benzekri Z, Arribou Z, Ech-chihbi E, Guo L, Dahmani K, Nouneh K, Briche S, Boukhris S, Cherkaoui M, (2021) A detailed investigation on the corrosion inhibition effect of by newly synthesized Pyran derivative on mild steel in 1.0 M HCl:

Experimental, surface morphological (SEM-EDS, DRX& AFM) and computational analysis (DFT & MD simulation), J. Mol. Liq, 344: 117777

[44] Ech-chihbi E, Nahlé A, Salim R, Benhiba F, Moussaif A, El-Hajjaji F, Oudda H, Guenbour A, Taleb M, Warad I, Zarrouk A (2020) Computational, MD simulation, SEM/EDX and experimental studies for understanding adsorption of benzimidazole derivatives as corrosion inhibitors in 1.0 M HCl solution, J. Alloys Compd, 844: 155842.

[45] Riffi O, Salim R, Ech-chihbi E, Taleb M, Fliou J, Elhourri M, Amechrouq A (2022) Experimental and quantum studies of Dysphania ambrosioïdes (L.) as ecological corrosion inhibitor for mild steel in hydrochloric acide environment, Journal of bio-and tribo-corrosion, 8:113

[46] Melian R, Radi M, Galai M, Ouakki M, Ech-chihbi E, Dkhirche N, Guo L, EbnTouhami M (2021) Anticorrosion properties of 5,5′-dithiobis-(2-nitrobenzoic acid) and sodium sulfite compounds for aluminum alloy 2024-T3 in saline solution: Electrochemical, characterization and theoretical investigations, J. Mol. Liq, 331: 115661